VARIOUS TYPES OF DRY FRICTION CHARACTERISTICS FOR VIBRATION DAMPING

Ladislav Půst*, Luděk Pešek*, Alena Radolfová*

Paper deals with derivation of mathematical relationships of dry friction force versus relative velocity in friction contact of two bodies. It is focused on such main types of dry friction characteristics, which frequently occur in dynamic mechanical systems. New models of modified Coulomb friction law and spring – friction elements are determined. For easy application in computing programs used in technical practice and based on linear equations, the equivalent linear stiffness and damping expressions are formulated and analysed in detail.

Keywords : *dry friction, stick-slip motion, modified Coulomb law, equivalent lineariza-tion, equivalent stiffness, equivalent damping coefficient*

1. Introduction

Dry friction forces are present in all machine structures and mechanisms, where they strongly influence both the energy dissipations and the dynamic behavior of the entire systems. The oscillations of systems with dry friction belong to the so called non-smooth strong nonlinear phenomena, where jumps in friction forces occur during motion. At certain conditions, the dry friction can cause instability and dangerous selfexcited vibrations.

Characteristics of dry friction i.e. a 'force-relative motion' relationship have been inten-sively investigated for more than two centuries both experimentally and analytically. The mathematical description of friction characteristics is of primary importance for analytical and numerical solutions and is often dependent on the quality of a mathematical model and on its ability to express the real mechanical structure properties.

The simple Coulomb dry friction law cannot describe a huge variety of real tribological phenomena. Therefore, many articles and books related to theoretical and experimental ap-proaches to friction properties have been published. Let us shortly mention some overviews of friction problems in [1, 2], special aspects of surface roughness [3, 4], application to turbine blade dampers [5–8], problems of surface wear [9, 10], friction at rolling [11], etc.

This article presents several main types of dry friction characteristics, which enable to describe and to calculate frequently occurred friction connections in dynamic mechanical systems. Program packets based on linear equations, the equivalent linear stiffness and damping expressions of friction characteristics derived in the first part are also added for easy computing.

* Ing. L. Půst, DrSc., Ing. L. Pešek, CSc., Ing. Mgr. A. Radolfová, Institute of Thermomechanics AS CR, v.v.i., Dolejškova 5, 18200 Praha 8

2. Characteristics of dry friction contacts

The simplest and also very frequently used description of dry friction force arising between two contacting and mutually moving surfaces of solid bodies is called Coulomb law (see Fig. 1):

$$
\begin{aligned}
F_{\mathrm{t}} &= f\,F_{\mathrm{N}}\,\mathrm{sgn}(v) = f\,F_{\mathrm{N}}\,\frac{v}{|v|} = f\,F_{\mathrm{N}}\,(H(v) - H(-v)) && \text{for} \quad v \neq 0 \;, \\
F_{\mathrm{t}} &\in \langle -f\,F_{\mathrm{N}}, f\,F_{\mathrm{N}} \rangle && \text{for} \quad v = 0 \;,
\end{aligned}
\tag{1}
$$

where f is the coefficient of dry friction, F_{N} normal force, v relative velocity, F_{t} friction force – positive in the sense of velocity*, $H(v)$ Heaviside function $H = 1$ for $v > 0$ and $H = 0$ for $v < 0$.

The first row of equation (1) expresses the force-velocity relationship in the slip phase of motion, the second row gives the interval of force, in which the relative velocity of bodies is zero – stick phase of contact.

The graph of Coulomb law where both phases of contact are drawn is in Fig. 1. Because the frictional drag of contact in the stick phase of loading before the beginning of motion is usually greater than during the slip phase of motion with non zero velocity, the Coulomb law is frequently modified by the addition of another second row in (1)

$$
F_{\mathrm{t}} \in \langle -f_{\mathrm{s}}\,F_{\mathrm{N}}, f_{\mathrm{s}}\,F_{\mathrm{N}} \rangle \;,
\tag{1a}
$$

where the static friction coefficient f_{s} in rest is greater than the dynamic friction coefficient f: $f_{\mathrm{s}} > f$. Graphical presentation of such a characteristic is in Fig. 2.
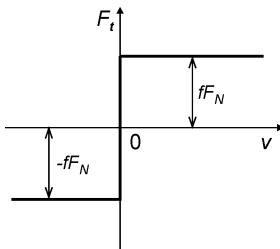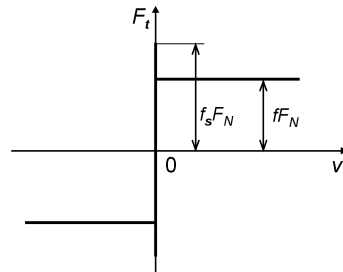

Fig.1

Fig.2

The transition from stick to slip phase of friction force-velocity characteristic is continuous without any jump for certain combinations of materials. The general description of such a nonlinear dry friction characteristic is

$$
\begin{aligned}
F_{\mathrm{t}} &= F_{\mathrm{N}}\,f(v)\,(H(v) - H(-v)) && \text{for} \quad v \neq 0 \;, \\
F_{\mathrm{t}} &\in \langle -f_{(0)}\,F_{\mathrm{N}}, f_{(0)}\,F_{\mathrm{N}} \rangle && \text{for} \quad v = 0 \;, \quad f_{(0)} = f_{\mathrm{s}} \;,
\end{aligned}
\tag{2}
$$

and it is depicted in Fig. 3.

Friction coefficient can also depend on the intensity of normal force F_{N}. Expressions (2) can also be used in this case, but the function $f(v)$ has to be replaced by a more complicated one $f(v, F_{\mathrm{N}})$.

---

* Friction force F_{t} is here taken positive for positive velocity v in conformity with [1], where the friction force is explained 'as the force to lift off the contacts of the upper surface over the contacts of the lower surface'.
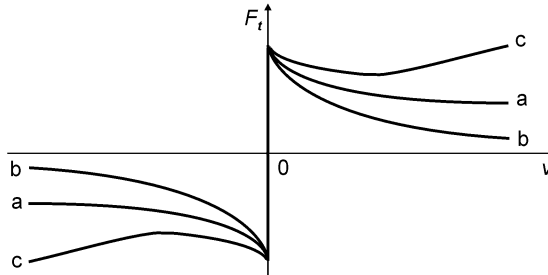
Fig.3

Relations (1) and (2) are exactly applicable for cases, in which the slipping bodies are very stiff so that the relative displacement of their centers of mass or places of measurement is the same as the relative displacements of contact surface points.

However, if there is any elastic connection between the center of mass (point of measurement) and the contact surface, than with an increase of friction force F_t from zero value in the range $|F_t| < f\, F_N$, the small elastic deformations occur first. It is not until the sliding force reaches the limit value of stick force, that the motion with velocity $|v| > 0$ begins. The simplified model of such a connecting element between points A, B is drawn in Fig. 4a. A model of the classical Coulomb element with a stiff connection between the friction surfaces and points of application of forces F_t is in Fig. 4b. Fig. 4c shows the scheme of a parallel connection of spring and damping in an equivalent linearized model (Chapter 4).
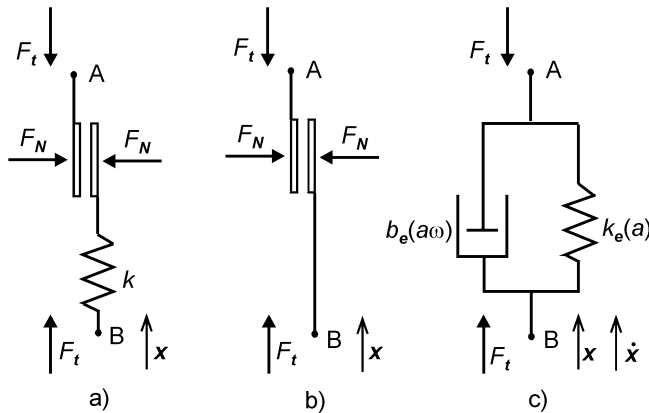

Fig.4

Courses of force F_t of spring-friction element at vibration (e.g. $x = x_0 \sin \omega t$) of points B against A are shown in Fig. 5. The start from origin $x = 0$, $\dot{x} = 0$ begins by linear increase of F_t along line 1, the stationary periodic process is represented by a rhomboid in the case of elastic micro-deformation (Fig. 5a) or by a rectangle for an infinitely stiff spring (Fig. 5b). Inclined or vertical lines correspond to the deformations of the spring at zero friction velocity (stick), horizontal sides of the figures illustrate relative motion (slip) in a friction element at constant deformation of spring.

Areas of figures are proportional to the dissipated energy during one cycle. In real conditions, sides of figures in Fig. 5 are not straight lines but general curves (see [8]) influenced both by general friction characteristics and nonlinear properties of spring.

Micro-deformations depicted by a inclined lines in Fig. 5a are caused mostly by elastic deformations of bodies near the friction surfaces, but they are also accompanied by partial microslips in several points of the contact area, where owing to non-uniform distribution of contact pressure a part of the area is less loaded or even without contact as it is evident e.g. from photos in [8].

Processes which happen during the stick period near the zero relative velocity are therefore always related to friction motions and are also highly influenced by wear, geometric precision, etc. Therefore their mathematical model is very uncertain.
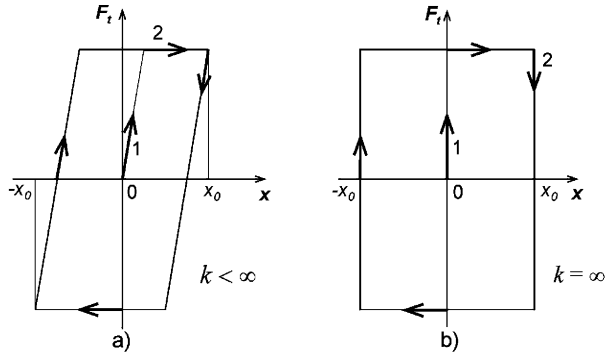

Fig.5

If it is taken into consideration that in extreme positions at vibrations and at low relative velocity the change of polarity of friction force lasts a short interval of time and that it is connected by a small dissipation of energy, then it is possible to model this short process approximately by an inclined line in the modified Coulomb diagram $F_t(v)$ and describe it mathematically by the following relationship

$$F_t = \frac{f\,F_N}{v_r}\,v \qquad \text{for} \quad |v| < v_r \ , \tag{3}$$

which replaces the second equation in (1). Threshold velocity v_r is seen in Fig. 3.

Such a modified Coulomb law can be described by one expression:

$$F_t = f\,F_N\left[\frac{v}{v_r}\left(1 - H(|v| - v_r)\right) + \text{sgn}(v)\,H(|v| - v_r)\right] \ . \tag{4}$$
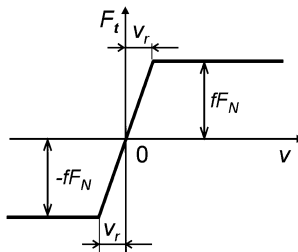
Its graphical representation is in Fig. 6.

Fig.6

At small relative velocities $|v| < v_\mathrm{r}$ the friction force F_t linearly increases to the value $f\,F_\mathrm{N}$. Then the full slip between both contact surfaces starts $|v| > v_\mathrm{r}$ and the friction force does not change $F_\mathrm{t} = \pm f\,F_\mathrm{N}$ in this whole slip phase of motion. Because, in a similar way as it is shown in Fig. 3, the friction force changes very often its magnitude with increasing velocity v, then it is important to introduce a general function $F_\mathrm{t}(v)$ into the equation (4). Such a description of general friction characteristic is

$$F_\mathrm{t} = F_\mathrm{t0}\,\frac{v}{v_\mathrm{r}}\,(1 - H(|v| - v_r)) + [F_\mathrm{t0}\,\mathrm{sgn}(v) + g(v - v_\mathrm{r}\,\mathrm{sgn}(v))]\,H(|v| - v_\mathrm{r})\;, \qquad (5)$$

which contains both the sudden change of friction force near the origin and the general course of nonlinear friction force $g(v)$ in the slip phase of motion. This function is continuous and can be expressed by a power series:

$$g(v_\mathrm{a}) = \sum_{n=1}^{N} b_n\,v_\mathrm{a}^n \qquad (6)$$

where $v_\mathrm{a} = v - v_\mathrm{r}\,\mathrm{sgn}(v)$.

Examples of such a friction characteristics are shown in the following figures for fixed values $|v| < v_\mathrm{r} = 0.5$, $F_\mathrm{t} = 1$ and for a power series of the fourth degree:

$$g(v_\mathrm{a}) = (b_1 + b_2\,|v_\mathrm{a}| + b_3\,v_\mathrm{a}^2 + b_4\,|v_\mathrm{a}|^3)\,v_\mathrm{a}\;. \qquad (7)$$

Friction characteristics with linear increase $b_1 = -0.1; 0; 0.1$ of friction force F_t is in Fig. 7.
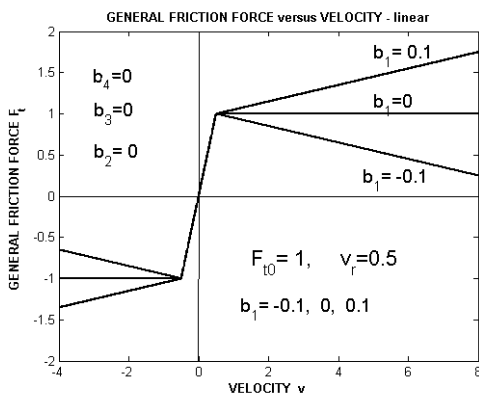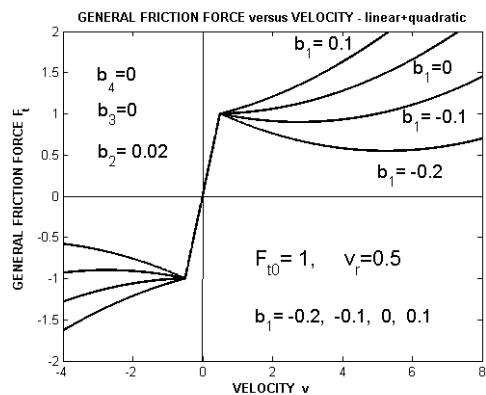

Fig.7   *Fig.8*

If only the first (linear) and the second (quadratic) members in $g(v_\mathrm{a})$ are used:

$$g(v_\mathrm{a}) = b_1\,v_\mathrm{a} + b_2\,|v_\mathrm{a}|\,v_\mathrm{a}\;, \qquad (8)$$

then the corresponding friction characteristics are plotted in Fig. 8 for $b_1 = 0.1; 0; -0.1; -0.2$ and $b_2 = 0.02$.

The stronger increase of friction slipping force is achieved by combining the first and the fourth power of relative velocity v_a. It is shown in Fig. 9 calculated for function

$$g(v_\mathrm{a}) = b_1\,v_\mathrm{a} + b_4\,|v_\mathrm{a}|^3\,v_\mathrm{a}\;, \qquad (9)$$

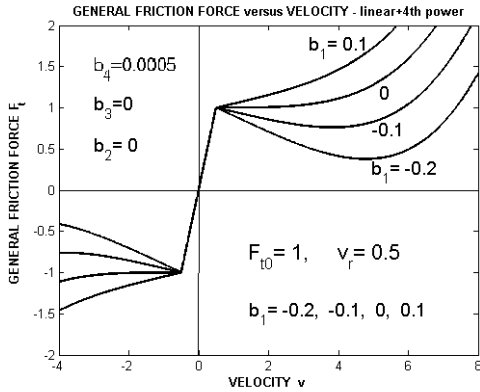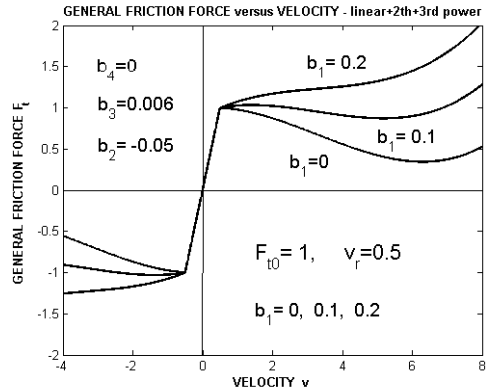where $b_4 = 0.0005$ and $b_1 = -0.2 \div 0.1$.

Fig.9

Fig.10

Both of these functions have the same sense of curvature in the whole interval $v > v_{\rm r}$. By means of appropriate combination of coefficients b_i in equation (7), it is possible to get partially concave and partially convex curvatures. Such a property is shown in Fig. 10 for the function

$$g(v_{\rm a}) = b_1\, v_{\rm a} + b_2\, |v_{\rm a}|\, v_{\rm a} + b_3\, v_{\rm a}^3 \ , \tag{10}$$

with the values $b_1 = 0; 0.1; 0.2$, $b_2 = -0.05$, $b_3 = 0.006$.

A mathematical model of friction characteristics with finite number of elements in power series form of function $g(v - v_{\rm r}\, {\rm sgn}(v))$ can only be used for a limited region of slip velocity v (or $v_{\rm a}$), because the magnitude of friction force increases with increasing $v_{\rm a}$ to infinity and does not describe the physical reality.

To express friction properly in the case, in which the friction force at great velocity v settles on a constant value, it is possible to use the functions $\arctan(v)$ or $\exp(-v)$. In Fig. 11 an example of such a course of friction characteristics is calculated with function

$$F_{\rm t} = F_{\rm N}\, f \left\{ \frac{v}{v_{\rm r}}\, (1 - H(|v| - v_{\rm r})) + [{\rm sgn}(v) + b_{\rm a}\, \arctan(v - v_{\rm r}\, {\rm sgn}(v))]\, H(|v| - v_{\rm r}) \right\} \tag{11}$$
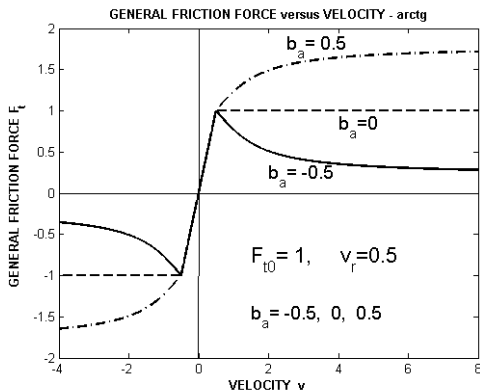
and $b_{\rm a} = -0.5; 0; 0.5$.
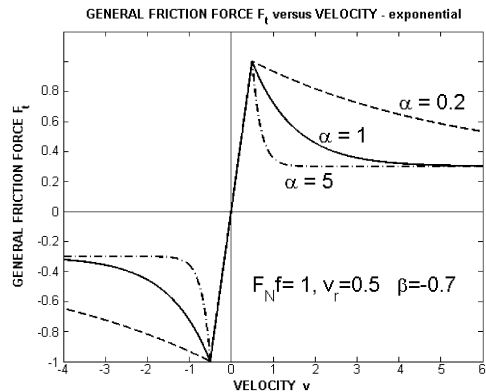

Fig.11

Fig.12

Fig. 12 shows three friction characteristics of the similar property as in the previous case, but instead of function arctan the exponential function is used:

$$F_t = F_N \, f \left\{ \frac{v}{v_r} \left(1 - H(|v| - v_r)\right) + \left[1 + \beta \left(1 - \exp(-\alpha \left(|v| - v_r\right))\right)\right] H(|v| - v_r) \right\} . \qquad (12)$$

Parameter β ascertains the value of friction force at very large slip velocity $F_t(v \to \infty) = = F_N \, f \, (1 + \beta)$ and parameter α determines the decline of friction characteristics in boundary crossing point $v = v_r$. The influence of this parameter on the course of friction characteristic is evident from Fig. 12, where $F_t(v)$ curves are plotted for $\alpha = 0.2; 1; 5$ at the same $\beta = -0.7$.

Different friction coefficient f_1 in the slip phase from the friction coefficient f_2 in the stick phase can be introduced into the mathematical friction models (1)–(10) very simply by applying two coefficients for ranges $|v| < v_r$ and $|v| > v_r$. Modified equation (4) is then

$$F_t = F_N \left[f_2 \frac{v}{v_r} \left(1 - H(|v| - v_r)\right) + f_1 \, \mathrm{sgn}(v) \, H(|v| - v_r) \right] \qquad (13)$$

and equation (5)

$$F_t = F_N \, f_2 \frac{v}{v_r} \left(1 - H(|v| - v_r)\right) + \left[F_N \, f_1 \, \mathrm{sgn}(v) + g(v - v_r \, \mathrm{sgn}(v))\right] H(|v| - v_r) . \qquad (13a)$$

An example of such a characteristic is in Fig. 13, where $F_{t0} = F_N \, f_1 = 1$, $F_{tk} = F_N \, f_2 = 2$ and the others parameters are the same as in the lower curve in Fig. 10, i.e. $b_1 = 0$, $b_2 = -0.05$, $b_3 = 0.006$, $b_4 = 0$.
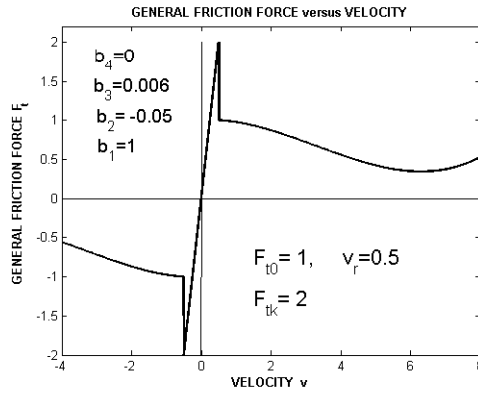
Fig.13

Different friction properties in stick and slip phase of motion can be modeled a similar way in other cases as well.

The arbitrary nonlinear friction characteristic can be mathematically described by a sum of piecewise-linear functions. The basic element of such a sum is plotted in Fig. 14 and expressed by

$$F_{tn} = b_n \left(v - v_{rn} \, \mathrm{sgn}(v)\right) H(|v| - v_{rn}) , \qquad (14)$$

where $b_n = \tan \beta_n$ is the slope of slip friction function beginning at $|v| = v_{rn}$.

GENERAL FRICTION FORCE F$_t$ versus VELOCITY - piecewise linear

Fig.14   Fig.15

Example of a characteristic consisting of 6 linear sections in region $v > 0$ is shown in Fig. 15.

This piecewise linear characteristic is given by

$$F_t(v, \mathbf{B}, \mathbf{V}) = \sum_{n=1}^{6} b_n \left(v - v_{rn} \, \mathrm{sgn}(v) \right) H(|v| - v_{rn}) \ , \tag{15}$$

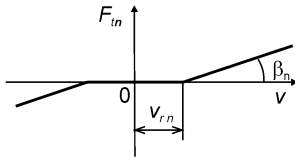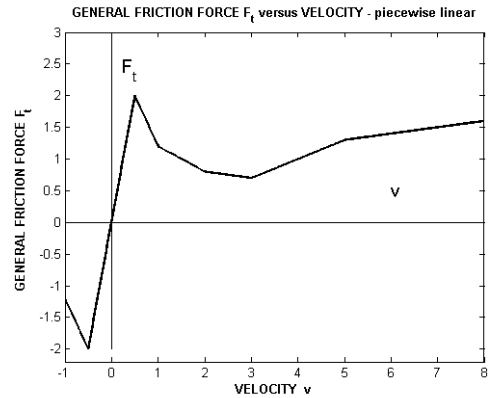where the parameters b_n, v_{rn} are elements of vectors $\mathbf{B}$, $\mathbf{V}$, which for the friction characteristic drawn in Fig. 15 are

$$\begin{aligned}
\mathbf{B} &= \begin{bmatrix} 4 & -5.6 & 1.2 & 0.3 & 0.4 & -0.2 \end{bmatrix} \ , \\
\mathbf{V} &= \begin{bmatrix} 0 & 0.5 & 1 & 2 & 3 & 5 \end{bmatrix} \ .
\end{aligned} \tag{16}$$

Since the number n of piecewise linear sections in (15), (16) is not limited, it is possible to describe mathematically a quite arbitrary course of friction forces as the function of relative velocity in the contact. Due to a simple linear form of the basic element (14) it also is comparatively simple to express equivalent linear damping for complicated friction forces.

3. Equivalent linearization of dry friction processes

The development of mechanical engineering is based to a large extent on treatment of many applied problems, where quantitative, first approximation results play the very important roles. If a method of equivalent linearization is applied to the nonlinear element, which is a part of a much larger linear mechanical system, the whole system can be treated as linear, which simplifies the solution of the problem.

The importance of an equivalent linearization method is supported by the fact that in the last decades a lot of commercial programme packets based on solutions of linear differential equations have been more and more employed.

For solving of technical problems it is often advantageous to replace strongly nonlinear friction characteristic by an equivalent linear function. Let us suppose that the displacement is near the harmonic oscillations $x = a \sin \omega t$ with velocity $\dot{x} = v = a \, \omega \, \cos \omega t$.

Equivalent linear damping coefficient $b_e(a \, \omega)$ [12, 13] is then

$$b_e(a \, \omega) = \frac{1}{\pi \, a \, \omega} \int_0^{2\pi} F_t(a \, \omega \, \cos \omega t) \, \cos \tau \, \mathrm{d}\tau \ , \tag{17}$$

where $a\,\omega = v_0$ is the amplitude of relative velocity between the friction surfaces. The course of one period of motion is in the time history $v(t)$ (in dimensionless form $v/v_{\mathrm{r}}(\tau)$) shown in Fig. 16.
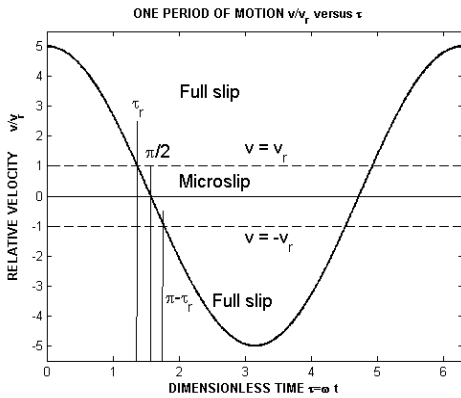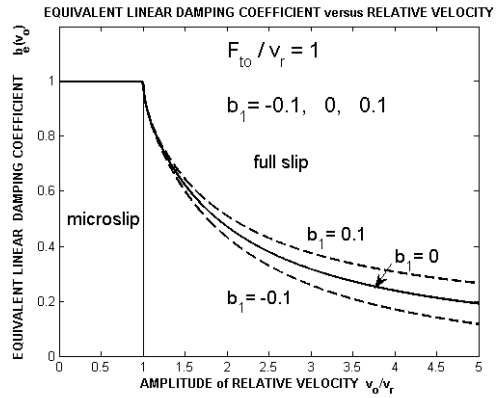

Fig.16

Fig.17

Instants of a transfer from full slip into microslip and reverse are in time τ_{r}, $\pi - \tau_{\mathrm{r}}$, $\pi + \tau_{\mathrm{r}}$, $2\pi - \tau_{\mathrm{r}}$, where

$$\tau_{\mathrm{r}} = \arccos\left(\frac{v_{\mathrm{r}}}{v_0}\right) \ . \tag{18}$$

Replacement of the modified Coulomb's law with the microslip (4) drawn in Fig. 6 by a linearized formula is realized by substituting $v = v_0 \cos\tau$ into (4) and (17) with view of (18):

$$b_{\mathrm{e}}(v_0) = \frac{F_{\mathrm{t}0}}{\pi\,v_0} \int_0^{2\pi} \left\{ \frac{v_0\,\cos\tau}{v_{\mathrm{r}}} \left[1 - H(|v_0\,\cos\tau| - v_{\mathrm{r}})\right] + \right.$$
$$\left. + \operatorname{sgn}(v_0\,\cos\tau)\,H(|v_0\,\cos\tau| - v_{\mathrm{r}}) \right\} \cos\tau\,\mathrm{d}\tau \ . \tag{19}$$

Due to the discontinuities of functions H and sgn it is necessary to solve this integral by parts with the time boundary τ_{r} shown in Fig. 16 and equation (18).

Integral interval 2π in (19) can be reduced to a quarter

$$\int_0^{2\pi} \{\ldots\} \cos\tau\,\mathrm{d}\tau = 4 \int_0^{\pi/2} \{\ldots\} \cos\tau\,\mathrm{d}\tau \ . \tag{19a}$$

At small amplitudes $v_0 < v_{\mathrm{r}}$, in which the motion exists only in the microslip domain, equivalent linear damping coefficient b_{e} is given by a slope of line going through the origin in Fig. 6:

$$b_{\mathrm{e}} = \frac{F_{\mathrm{t}0}}{v_{\mathrm{r}}} \qquad \text{for} \quad v_0 < v_{\mathrm{r}} \ . \tag{20}$$

The values $\cos\tau_{\mathrm{r}} = v_{\mathrm{r}}/v_0$ are real and smaller (or equal) than 1 at greater velocity amplitudes $v_0 \geq v_{\mathrm{r}}$. Dimensionless transition time τ_{r} is smaller than $\pi/2$. The friction

contact passes during one cycle both microslip and full slip domain. For $v_0 > v_\mathrm{r}$ the equivalent linear damping coefficient is:

$$b_\mathrm{e}(v_0) = \frac{4}{\pi} F_\mathrm{t0} \left[\int_0^{\tau_\mathrm{r}} \frac{1}{v_0} \cos \tau \, \mathrm{d}\tau + \int_{\tau_r}^{\pi/2} \frac{1}{v_\mathrm{r}} \cos^2 \tau \, \mathrm{d}\tau \right] =$$

$$= \frac{4\,F_\mathrm{t0}}{\pi\,v_\mathrm{r}} \left[\frac{v_\mathrm{r}}{v_0} \sin \tau_r + \frac{\pi}{4} - \frac{\tau_\mathrm{r}}{2} - \frac{1}{4} \sin 2\tau_\mathrm{r} \right] \ . \tag{21}$$

This formula can be simplified by using the relationship (18):

$$b_\mathrm{e}(v_0) = \frac{F_\mathrm{t0}}{v_\mathrm{r}} \left[1 - \frac{2\,\tau_\mathrm{r}}{\pi} + \frac{\sin 2\tau_\mathrm{r}}{\pi} \right] \ . \tag{22}$$

It is also possible to express $b_\mathrm{e}(v_0)$ as function of only velocity amplitude:

$$b_\mathrm{e}(v_0) = \frac{F_\mathrm{t0}}{v_\mathrm{r}} \left[1 - \frac{2}{\pi} \arccos \left(\frac{v_\mathrm{r}}{v_0} \right) + \frac{2}{\pi} \frac{v_\mathrm{r}}{v_0} \sqrt{1 - \left(\frac{v_\mathrm{r}}{v_0} \right)^2} \right] \ . \tag{23}$$

Equations (20)–(23) describing the relationship of equivalent linear damping coefficient b_e on velocity amplitude v_0 and replacing the friction characteristics drawn in Fig. 6 are graphically represented in Fig. 17 by a solid line – $b_1 = 0$. The course of equivalent damping coefficient $b_\mathrm{e}(v_0)$ for the dry friction combined with linear damping (Fig. 7) is in Fig. 17 depicted by dashed curves for $b_1 = -0.1$ and $b_1 = 0.1$.

The advantage of including microslip phase into the classical friction Coulomb law is not only in its better comprehension of real physical processes in friction surfaces at small displacements, but also in the easier mathematical modelling and computation, because the equivalent damping b_e has limited value $b_\mathrm{e}(v_0) \leq F_0/v_\mathrm{r}$, whereas the classical Coulomb law without microslip gives at $v_0 \to 0$ infinitely high value of equivalent linear damping $b_\mathrm{e} \approx 1/v_0 \to \infty$, unsuitable for calculation.

In a similar way it is possible to determine equivalent linear damping coefficient b_e also for the more general friction characteristics shown e.g. in Figs 7–10. All these characteristics contain three main parts, two of them are: linear increase of force in interval $-v_\mathrm{r} \leq v \leq v_\mathrm{r}$ and constant value in interval $|v| > v_\mathrm{r}$. The relationships (17)–(23) derived earlier can be used for these parts.

The third parts of the mentioned characteristics in Figs 7–10 contain several power functions v^n, $n = 1, 2, 3, 4$. Corresponding equivalent damping expressions are derived in the following text.

For linear increase of friction force $b_1 v_\mathrm{a} = b_1 (v - v_\mathrm{r} \, \mathrm{sgn}(v))$ and for $v = v_0 \cos\tau$, $v_0 > v_\mathrm{r}$, $0 < \tau < \tau_\mathrm{r}$ the equivalent damping coefficient is

$$b_\mathrm{e1}(v_0) = \frac{4\,b_1}{\pi\,v_0} \int_0^{\tau_\mathrm{r}} (v_0 \cos \tau - v_\mathrm{r}) \cos \tau \, \mathrm{d}\tau =$$

$$= \frac{4\,b_1}{\pi} \left(\frac{\tau_\mathrm{r}}{2} - \frac{1}{4} \sin 2\tau_\mathrm{r} \right) = \frac{2\,b_1}{\pi} \left[\arccos \left(\frac{v_\mathrm{r}}{v_0} \right) - \frac{v_\mathrm{r}}{v_0} \sqrt{1 - \left(\frac{v_\mathrm{r}}{v_0} \right)^2} \right] \ . \tag{24}$$

In the case of quadratic function $b_2\, v_{\mathrm{a}}\, |v_{\mathrm{a}}| = b_2\,(v_0\,\cos\tau - v_{\mathrm{r}})\,|v_0\,\cos\tau - v_{\mathrm{r}}|$, this coefficient is

$$
\begin{aligned}
b_{\mathrm{e}2}(v_0) &= \frac{4\,b_2}{\pi\,v_0} \int\limits_0^{\tau_{\mathrm{r}}} (v_0\,\cos\tau - v_{\mathrm{r}})^2\,\cos\tau\,\mathrm{d}\tau = \\
&= \frac{4\,b_2}{\pi\,v_0}\left[v_0^2\left(\sin\tau_{\mathrm{r}} - \frac{\sin^3\tau_{\mathrm{r}}}{3}\right) - 2\,v_0\,v_{\mathrm{r}}\left(\frac{\tau_{\mathrm{r}}}{2} + \frac{1}{4}\,\sin 2\tau_{\mathrm{r}}\right) + v_{\mathrm{r}}^2\,\sin\tau_{\mathrm{r}}\right] = \\
&= \frac{4\,b_2\,v_0}{\pi}\left[-\frac{v_{\mathrm{r}}}{v_0}\,\tau_{\mathrm{r}} + \left(1 + \frac{v_{\mathrm{r}}^2}{v_0^2}\right)\sin\tau_{\mathrm{r}} - \frac{1}{2}\,\frac{v_{\mathrm{r}}}{v_0}\,\sin 2\tau_{\mathrm{r}} - \frac{1}{3}\,\sin^3\tau_{\mathrm{r}}\right] = \\
&= \frac{4\,b_2\,v_{\mathrm{r}}}{\pi}\left[-\tau_{\mathrm{r}} + \frac{v_0}{v_{\mathrm{r}}}\,\sin\tau_{\mathrm{r}} - \frac{v_0}{3\,v_{\mathrm{r}}}\,\sin^3\tau_{\mathrm{r}}\right] \; ,
\end{aligned}
\tag{25}
$$

which can be again transposed onto the function of the variable v_{r}/v_0:

$$
b_{\mathrm{e}2}(v_0) = \frac{4\,b_2\,v_r}{\pi}\left[-\arccos\left(\frac{v_r}{v_0}\right) + \left(\frac{2}{3}\,\frac{v_0}{v_{\mathrm{r}}} + \frac{1}{3}\,\frac{v_{\mathrm{r}}}{v_0}\right)\sqrt{1 - \left(\frac{v_r}{v_0}\right)^2}\,\right] \; .
\tag{25a}
$$

Cubic element $b_3\, v_{\mathrm{a}}^3$ in equation (7) increases the equivalent linear damping coefficient $b_{\mathrm{e}}(v_0)$ on addition

$$
\begin{aligned}
b_{\mathrm{e}3}(v_0) &= \frac{4\,b_3}{\pi\,v_0} \int\limits_0^{\tau_{\mathrm{r}}} [v_0\,\cos\tau - v_{\mathrm{r}}]^3\,\cos\tau\,\mathrm{d}\tau = \\
&= \frac{4\,b_3\,v_r^2}{\pi}\left[\frac{v_0^2}{v_{\mathrm{r}}^2}\left(\frac{3}{8}\,\tau_{\mathrm{r}} + \frac{1}{4}\,\sin 2\tau_{\mathrm{r}} + \frac{1}{32}\,\sin 4\tau_{\mathrm{r}}\right) - \right. \\
&\qquad\qquad \left. - 3\,\frac{v_0}{v_{\mathrm{r}}}\left(\sin\tau_{\mathrm{r}} - \frac{1}{3}\,\sin^3\tau_{\mathrm{r}}\right) + \frac{3}{2}\left(\tau_{\mathrm{r}} + \frac{1}{2}\,\sin 2\tau_{\mathrm{r}}\right) - \frac{v_{\mathrm{r}}}{v_0}\,\sin\tau_{\mathrm{r}}\right] = \\
&= \frac{b_3\,v_{\mathrm{r}}^2}{\pi}\left[\frac{3}{2}\left(4 + \frac{v_0^2}{v_{\mathrm{r}}^2}\right)\tau_{\mathrm{r}} - 4\left(3\,\frac{v_0}{v_{\mathrm{r}}} + \frac{v_{\mathrm{r}}}{v_0}\right)\sin\tau_{\mathrm{r}} + \right. \\
&\qquad\qquad \left. + \left(\frac{v_0^2}{v_{\mathrm{r}}^2} + 3\right)\sin 2\tau_{\mathrm{r}} + \frac{1}{8}\,\frac{v_0^2}{v_{\mathrm{r}}^2}\,\sin 4\tau_{\mathrm{r}} + 4\,\frac{v_0}{v_{\mathrm{r}}}\,\sin^3\tau_{\mathrm{r}}\right] \; .
\end{aligned}
\tag{26}
$$

Component $b_{\mathrm{e}3}(v_0)$ can again be expressed as a function of ratio v_{r}/v_0 instead of transition time τ_{r}. This transformation based on relationship $v_{\mathrm{r}}/v_0 = \cos\tau_{\mathrm{r}}$ gives

$$
b_{\mathrm{e}3}(v_0) = \frac{b_3\,v_{\mathrm{r}}^2}{\pi}\left[\frac{3}{2}\left(4 + \frac{v_0^2}{v_{\mathrm{r}}^2}\right)\arccos\left(\frac{v_{\mathrm{r}}}{v_0}\right) - \sqrt{\left(1 - \frac{v_{\mathrm{r}}^2}{v_0^2}\right)}\left(6.5\,\frac{v_0}{v_{\mathrm{r}}} + \frac{v_{\mathrm{r}}}{v_0}\right)\right] \; .
\tag{26a}
$$

Component $b_{\mathrm{e}4}(v_0)$ of equivalent damping coefficient $b_{\mathrm{e}}(v_0)$, which corresponds to the fourth power element $b_4\,|v_{\mathrm{a}}|^3\,v_{\mathrm{a}}$ in nonlinear friction characteristic $F_{\mathrm{t}}(v_0)$, can be calculated again applying the integral formula (17):

$$
\begin{aligned}
b_{\mathrm{e}4}(v_0) &= \frac{b_4}{\pi\,v_0} \int\limits_0^{2\pi} |v - \operatorname{sgn} v_{\mathrm{r}}|^3\,(v - \operatorname{sgn} v_{\mathrm{r}})\,H(|v| - v_{\mathrm{r}})\,\cos\tau\,\mathrm{d}\tau = \\
&= \frac{4\,b_4}{\pi\,v_0} \int\limits_0^{\tau_{\mathrm{r}}} (v_0\,\cos\tau - v_{\mathrm{r}})^4\,\cos\tau\,\mathrm{d}\tau \; ,
\end{aligned}
\tag{27}
$$

which after integration and a small rearrangement gives

$$
b_{\text{e4}}(v_0) = \frac{b_4\, v_{\text{r}}^3}{\pi} \left[\left(-6\,\frac{v_0^2}{v_{\text{r}}^2} - 8\right) \tau_{\text{r}} + 4 \left(\frac{v_0^3}{v_{\text{r}}^3} + 6\,\frac{v_0}{v_{\text{r}}} + \frac{v_{\text{r}}}{v_0}\right) \sin\tau_{\text{r}} - 4 \left(\frac{v_0^2}{v_{\text{r}}^2} + 1\right) \sin 2\tau_{\text{r}} + \right.
$$
$$
\left. -\frac{1}{2}\,\frac{v_0^2}{v_{\text{r}}^2}\sin 4\tau_{\text{r}} - \left(\frac{8}{3}\,\frac{v_0^3}{v_{\text{r}}^3} + 8\,\frac{v_0}{v_{\text{r}}}\right)\sin^3\tau_{\text{r}} + \frac{4}{5}\,\frac{v_0^3}{v_{\text{r}}^3}\sin^5\tau_{\text{r}} \right] . \tag{28}
$$

Formula (28), which depends on time τ_{r}, can be again transformed into the function of velocity amplitude v_0 with result:

$$
b_{\text{e4}}(v_0) = \frac{b_4\, v_{\text{r}}^3}{\pi} \left[-\left(6\,\frac{v_0^2}{v_{\text{r}}^2} + 8\right)\arccos\left(\frac{v_{\text{r}}}{v_0}\right) + \right.
$$
$$
\left. + \frac{1}{15}\left(32\,\frac{v_0^3}{v_{\text{r}}^3} + 166\,\frac{v_0}{v_{\text{r}}} + 12\,\frac{v_{\text{r}}}{v_0}\right)\sqrt{1 - \left(\frac{v_{\text{r}}}{v_0}\right)^2} \right] . \tag{28a}
$$

General formula for equivalent linear damping coefficient $b_{\text{e}}(v_0)$, in which all partial expressions of $b_{\text{e1}}, \ldots, b_{\text{e4}}$ are used, enables to replace a general nonlinear friction characteristic $F_{\text{t}}(v)$

$$
F_{\text{t}} = F_{\text{N}}\, f\, \frac{v}{v_{\text{r}}}(1 - H(|v| - v_{\text{r}})) + [F_{\text{N}}\, f\, \text{sgn}(v) + b_1\,(v - v_{\text{r}}\,\text{sgn}(v)) +
$$
$$
+ b_2\,|v - v_{\text{r}}\,\text{sgn}(v)|\,(v - v_{\text{r}}\,\text{sgn}(v)) + b_3\,(v - v_{\text{r}}\,\text{sgn}(v))^3 + \tag{29}
$$
$$
+ b_4\,|(v - v_{\text{r}}\,\text{sgn}(v))|^3\,(v - v_{\text{r}}\,\text{sgn}(v))]\, H(|v| - v_{\text{r}})
$$

by a simple linear expression

$$
F_{\text{t}} = b_{\text{e}}(v_0)\, v . \tag{29a}
$$

The general formula for coefficient $b_{\text{e}}(v_0)$ in the last equation is

$$
b_{\text{e}}(v_0) = \frac{F_{\text{N}}\, f}{v_{\text{r}}}(1 - H(|v_0| - v_{\text{r}})) +
$$
$$
+ \frac{F_{\text{N}}\, f}{v_{\text{r}}}\left[1 - \frac{2}{\pi}\arccos\left(\frac{v_{\text{r}}}{v_0}\right) + \frac{2}{\pi}\,\frac{v_{\text{r}}}{v_0}\sqrt{1 - \left(\frac{v_{\text{r}}}{v_0}\right)^2}\right] H(|v_0| - v_{\text{r}}) +
$$
$$
+ \left[\frac{b_1}{\pi}\,2\left(\arccos\left(\frac{v_{\text{r}}}{v_0}\right) - \frac{v_{\text{r}}}{v_0}\sqrt{1 - \left(\frac{v_{\text{r}}}{v_0}\right)^2}\right) + \right.
$$
$$
+ \frac{4\,b_2\,v_{\text{r}}}{\pi}\left(-\arccos\left(\frac{v_{\text{r}}}{v_0}\right) + \left(\frac{v_0}{v_{\text{r}}}\,\frac{2}{3} + \frac{1}{3}\,\frac{v_{\text{r}}}{v_0}\right)\sqrt{1 - \left(\frac{v_{\text{r}}}{v_0}\right)^2}\right) + \tag{30}
$$
$$
+ \frac{b_3\,v_{\text{r}}^2}{\pi}\left(\frac{3}{2}\left(4 + \frac{v_0^2}{v_{\text{r}}^2}\right)\arccos\left(\frac{v_{\text{r}}}{v_0}\right) - \left(6.5\,\frac{v_0}{v_{\text{r}}} + \frac{v_{\text{r}}}{v_0}\right)\sqrt{1 - \left(\frac{v_{\text{r}}}{v_0}\right)^2}\right) +
$$
$$
+ \frac{b_4\,v_{\text{r}}^3}{\pi}\left(-\left(6\,\frac{v_0^2}{v_{\text{r}}^2} + 8\right)\arccos\left(\frac{v_{\text{r}}}{v_0}\right) + \right.
$$
$$
\left. + \frac{1}{15}\left(32\,\frac{v_0^3}{v_{\text{r}}^3} + 166\,\frac{v_0}{v_{\text{r}}} + 12\,\frac{v_{\text{r}}}{v_0}\right)\sqrt{1 - \left(\frac{v_{\text{r}}}{v_0}\right)^2}\right)\right] H(|v_0| - v_r).
$$

4. Examples of equivalent linear damping coefficients

The relationships for equivalent linear coefficients of damping that were derived in the previous chapter are very complicated and therefore it is useful to complete them by a graphical representation. Following figures should show the contribution of individual elements of friction characteristics to the course of equivalent linear damping coefficient $b_e(v_0)$.

The majority of the given diagrams (Figs 18–21) is calculated for the same parameters of microslip phase $F_{t0} = F_N f = 1$, $v_r = 0.5$, and an only diagram in Fig. 22 is calculated for a different friction coefficient in microslip and in full slip phase of motion.
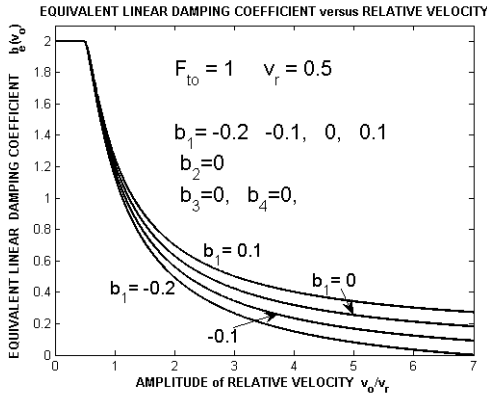
Fig.18
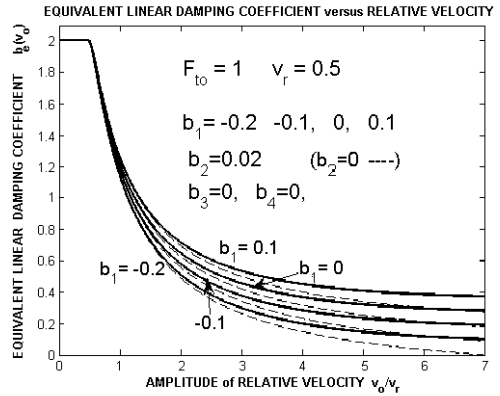
Fig.19

Courses of coefficient $b_e(v_0)$ depicted in Fig. 18 correspond to friction characteristics in Fig. 7, in which the relationships $F_t(v)$ in the full slip regions $|v| > v_r$ are linear with different slope b_1 and are described by :

$$F_t = [F_{t0} \, \text{sgn}(v) + b_1 \, (v - v_r \, \text{sgn}(v))] \, H(|v| - v_r) \,. \tag{31}$$

Damping coefficient is $b_e(v_0) = 2$ for $v_0 < v_r$ and for $v_0 > v_r$ it is

$$
b_e(v_0) = \frac{F_{t0}}{v_r} \left[1 - \frac{2}{\pi} \arccos\left(\frac{v_r}{v_0}\right) - \frac{2}{\pi} \frac{v_r}{v_0} \sqrt{1 - \left(\frac{v_r}{v_0}\right)^2} \right] +
$$
$$
+ \frac{2}{\pi} b_1 \left[\arccos\left(\frac{v_r}{v_0}\right) - \frac{v_r}{v_0} \sqrt{1 - \left(\frac{v_r}{v_0}\right)^2} \right] \,. \tag{32}
$$

In the region $v - v_r > 0$ it has a hyperbolic fall, which in the limit case $v_0 \to \infty$ and for $b_1 = -0.1; 0; 0.1$ goes to $b_e(\infty) = -0.1; 0; 0.1$. However, for negative b_1, equivalent coefficient be changes its sign at certain v_0 and the system becomes unstable. Such a situation happens for $b_1 = -0.2$ at $v_0/v_r \cong 7$ as seen in Fig. 18.

Characteristics $F_t(v)$ in Fig. 8 contain, besides Coulomb friction and linear damping, also quadratic function $b_2 |v_a| v_a$, in which $b_1 = -0.2 \div 0.1$, $b_2 = 0.02$. Corresponding curves of equivalent damping coefficients $b_e(v_0)$ are plotted in Fig. 19 for the same combinations of coefficients b_1, b_2. These curves are described by formulas

$$b_e = \frac{F_{t0}}{v_r} = 2 \qquad \text{for} \quad v_0 \le v_r$$

and by

$$
b_{\mathrm{e}}(v_0) = \frac{F_{\mathrm{t}0}}{v_{\mathrm{r}}} \left[1 - \frac{2}{\pi} \arccos\left(\frac{v_{\mathrm{r}}}{v_0}\right) - \frac{2}{\pi} \frac{v_{\mathrm{r}}}{v_0} \sqrt{1 - \left(\frac{v_{\mathrm{r}}}{v_0}\right)^2} \right] +
$$

$$
+ \frac{2}{\pi} \left[b_1 \left(\arccos\left(\frac{v_{\mathrm{r}}}{v_0}\right) - \frac{v_{\mathrm{r}}}{v_0} \sqrt{1 - \left(\frac{v_r}{v_0}\right)^2} \right) + \right. \tag{33}
$$

$$
\left. + 2 b_2\, v_{\mathrm{r}} \left(-\arccos\left(\frac{v_{\mathrm{r}}}{v_0}\right) + \left(\frac{v_0}{v_{\mathrm{r}}} \frac{2}{3} + \frac{1}{3} \frac{v_{\mathrm{r}}}{v_0}\right) \sqrt{1 - \left(\frac{v_{\mathrm{r}}}{v_0}\right)^2} \right) \right] \quad \text{for} \quad v_0 > v_{\mathrm{r}} \ .
$$

Two sets of curves are drawn in Fig. 19. Bold solid curves belong to non-zero coefficient $b_2 = 0.02$, the thin dashed curves depict equivalent damping coefficients $b_{\mathrm{e}}(v_0)$ for $b_2 = 0$. It is obvious that the quadratic element $b_2 |v_{\mathrm{a}}| v_{\mathrm{a}}$, $v_{\mathrm{a}} = v - v_{\mathrm{r}} \operatorname{sgn}(v)$ heightens damping and stabilizes motion, which at negative $b_1 < 0$ can be unstable over a certain threshold.

Friction connections with more progressive increasing of friction forces in the slip phase have similar curves of $b_{\mathrm{e}}(v_0)$ as seen in Fig. 20, in which the influence of the fourth power of slip velocity $b_4\, v_{\mathrm{a}}^4 = b_4\, (v - v_{\mathrm{r}}\, \operatorname{sgn}(v))^4$, $b_4 = 0.0005$ is demonstrated. Corresponding friction characteristics $F_{\mathrm{t}}(v)$ are shown in Fig. 9. Equivalent linear damping coefficient $b_{\mathrm{e}}(v_0)$ is at vibration with small amplitudes $v_0 \leq v_{\mathrm{r}}$ again constant $b_{\mathrm{e}}(v_0) = F_{\mathrm{t}0}/v_{\mathrm{r}} = 2$, at higher velocity amplitudes $v_0 > v_{\mathrm{r}}$ it strongly falls and it is described by relationship

$$
b_{\mathrm{e}}(v_0) = \frac{F_{\mathrm{N}}\, f}{v_{\mathrm{r}}} \left[1 - \frac{2}{\pi} \arccos\left(\frac{v_{\mathrm{r}}}{v_0}\right) + \frac{2}{\pi} \frac{v_{\mathrm{r}}}{v_0} \sqrt{1 - \left(\frac{v_{\mathrm{r}}}{v_0}\right)^2} \right] +
$$

$$
+ \frac{b_1}{\pi} 2 \left[\arccos\left(\frac{v_{\mathrm{r}}}{v_0}\right) - \frac{v_{\mathrm{r}}}{v_0} \sqrt{1 - \left(\frac{v_{\mathrm{r}}}{v_0}\right)^2} \right] + \tag{34}
$$

$$
+ \frac{b_4\, v_{\mathrm{r}}^3}{\pi} \left[-\left(6 \frac{v_0^2}{v_{\mathrm{r}}^2} + 8\right) \arccos\left(\frac{v_{\mathrm{r}}}{v_0}\right) + \frac{1}{15}\left(32 \frac{v_0^3}{v_{\mathrm{r}}^3} + 166 \frac{v_0}{v_{\mathrm{r}}} + 12 \frac{v_{\mathrm{r}}}{v_0}\right) \sqrt{1 - \left(\frac{v_{\mathrm{r}}}{v_0}\right)^2} \right] \ .
$$

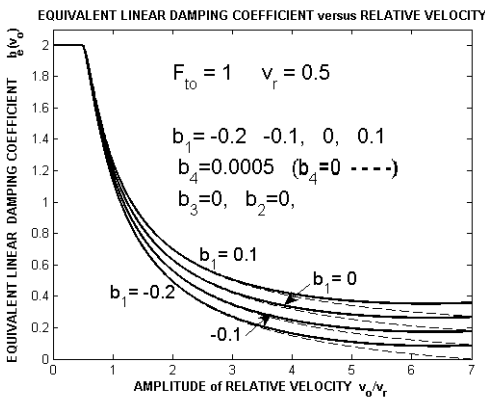
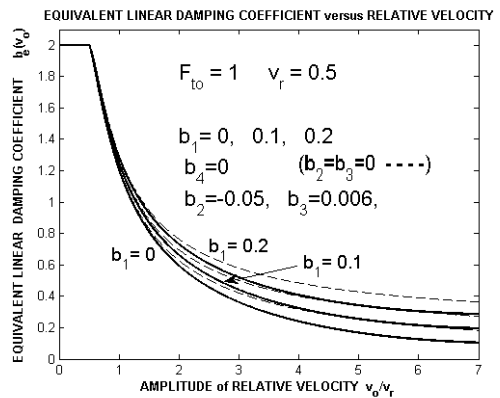*Fig.20*   *Fig.21*

Comparing Fig. 19 and Fig. 20 it is evident that the influence of quadratic power damping ($b_2 |v_a| v_a$, Fig. 19) is remarkable at smaller velocity $v_0/v_r \approx 2$ by diversity of courses without ($b_2 = 0$) and with quartic element ($b_2 = 0.02$). The influence of quartic velocity damping element ($b_4 |v_a|^3 v_a$, Fig. 20) is remarkable by splitting curves with and without this damping element till at twice higher velocity $v_0/v_r \approx 4$.

At $v_0/v_r = 7$ the differences between solid and dashed curves are equal in both cases, but at higher velocities v_0 the influence of quartic element $b_4 |v_a|^3 v_a$ increases more intensively.

The fundamental property of these relationships in Fig. 19 and 20 is their bending to the upper values, so that any instability in both cases for parameters given in the figures cannot occur.

Further example of practicable friction characteristic is drawn in Fig. 10, in which both concave and convex parts exist. Corresponding courses of equivalent damping coefficient $b_e(v_0)$ are described by expression

$$
\begin{aligned}
b_e(v_0) = {} & \frac{F_N \, f}{v_r} \left[1 - \frac{2}{\pi} \arccos\left(\frac{v_r}{v_0}\right) + \frac{1}{\pi} \frac{v_r}{v_0} \sqrt{1 - \left(\frac{v_r}{v_0}\right)^2} \right] + \\
& + \frac{b_1}{\pi} 2 \left[\arccos\left(\frac{v_r}{v_0}\right) - \frac{v_r}{v_0} \sqrt{1 - \left(\frac{v_r}{v_0}\right)^2} \right] + \\
& + \frac{4 \, b_2 \, v_r}{\pi} \left[-\arccos\left(\frac{v_r}{v_0}\right) + \left(\frac{v_0}{v_r} \frac{2}{3} + \frac{1}{3} \frac{v_r}{v_0}\right) \sqrt{1 - \left(\frac{v_r}{v_0}\right)^2} \right] + \\
& + \frac{b_3 \, v_r^2}{\pi} \left[\frac{2}{3} \left(4 + \frac{v_0^2}{v_r^2}\right) \arccos\left(\frac{v_r}{v_0}\right) - \left(6.5 \frac{v_0}{v_r} + \frac{v_r}{v_0}\right) \sqrt{1 - \left(\frac{v_r}{v_0}\right)^2} \right] .
\end{aligned}
\tag{35}
$$

Differences in courses friction characteristics $F_t(v)$ shown in Figs 7–10 and connected with the variations of parameters $b_1 \div b_4$ are very marked. In spite of this, these variations manifest themselves in the courses of equivalent damping coefficients $b_e(v_0)$ much weakly as it is evident from Figs 18–21. Therefore identification construction of mathematical model of friction characteristics $F_t(v)$ from experimentally determined equivalent damping coefficients $b_e(v_0)$ (or from energy-less, from hysteresis loop) is very difficult due to measurements errors, but it is a possible way how to improve description of friction processes.

Description of friction characteristic by means of power series of relative velocity v is not the single one. Further way of description of general course of friction process is the application of piecewise linear functions. Such a function was used in equations (15), (16) and graphically presented in Fig. 15.

At derivation of equivalent linear damping coefficient $b_e(v_0)$ it is possible to use a superposition principle of sectional damping coefficients $b_e(v_0)$ belonging to a partial friction function (14) depicted in Fig. 14. According to equation (24) it is

$$
\begin{aligned}
b_{en}(v_0) &= \frac{2 \, b_n}{\pi} \left[\arccos\left(\frac{v_{rn}}{v_0}\right) - \frac{v_{rn}}{v_0} \sqrt{1 - \left(\frac{v_{rn}}{v_0}\right)^2} \right] && \text{for} \quad v_0 > v_{rn} \ , \\
b_{en}(v_0) &= 0 && \text{for} \quad v_0 \le v_{rn} \ .
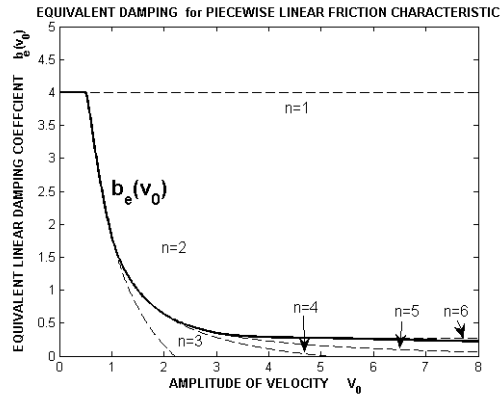\end{aligned}
\tag{36}
$$

Fig.22

In Fig. 22, as an example of superposition of these formulae, the equivalent linear damping coefficient $b_e(v_0)$ corresponding to the friction force characteristic in Fig. 15 is shown

$$b_e(v_0) = \sum_{n=1}^{6} b_{en}(v_0) \ . \tag{37}$$

Equation (37) is drawn in Fig. 22 by a solid thick line, individual contributions (36) are limited by dashed thin lines and are labelled by $n = 1 \div 6$. These areas begin at the points given by velocity amplitudes v_{rn} – elements of vector $\mathbf{V}$ in equation (16):

$$v_0 = v_{rn} = 0; 0.5; 1; 2; 3; 5 \ . \tag{38}$$

A similar procedure of calculation of equivalent linear damping coefficients $b_e(v_0)$ can also be applied by replacements of friction characteristics containing functions arctan or exp (see equations (11), (12), Figs 11, 12) by linear expressions. Necessary integral transformations are e.g. in [15].

5. Friction contact with elastic micro-deformations

In previous chapters friction characteristics were described by a single expression in the range of small velocities, in which meets the case when the elastic micro-deformations of bodies near the contact areas of friction connection are very small. Mathematical expression of these force-deformation processes at small relative velocities near the reverse of sense of motion is, according to equation (4) and Fig. 6, based on a substitute expression as viscous linear relationship of friction force F_t in the region $v \in (-v_r, +v_r)$, where v_r is a small relative velocity. Due to application of only one variable this replacement is – common for small and high relative velocities – comparatively simple and enables easy calculation for a majority of engineering problems, where the stiff vibrating bodies contact and shear each other.

However at some friction couples, where friction surfaces are placed on some relative compliant parts of moving bodies, – see e.g. Fig. 23 – there it is necessary to use more sophisticated computational model.

Because the relative motion of solid body $x(t)$ slightly differs from the motion $x_1(t)$ in friction area due to the elastic deformation of body's bulge, it is possible to model such a contact according to the Fig. 24.
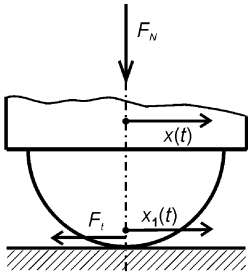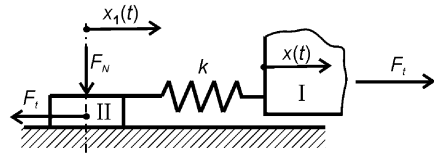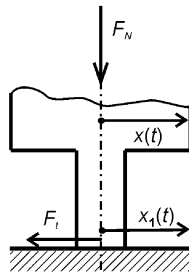
Fig.23   Fig.24

Let us solve motion of this system at assumption of classical Coulomb friction (Fig. 1) and of the prescribed excitation harmonic motion of body I $x(t) = a \cos \omega t$ with the initial conditions: $x(0) = a$, $x_1(0) = a - f F_N/k$, $\dot{x}(0) = 0$, $\dot{x}_1(0) = 0$, $F_t(0) = f F_N$, which are in agreement with stationary periodic motion. Motion of friction contact II is non-harmonic with non-smooth velocity. Course of displacement $x_1(t)$ is given by

$$x_1 = a - \frac{f F_N}{k} \qquad t \in (0, t_r) , \qquad\qquad x_1 = a \cos \omega t + \frac{f F_N}{k} \qquad t \in \left(t_r, \frac{T}{2}\right) ,$$
$$x_1 = -a + \frac{f F_N}{k} \qquad t \in \left(\frac{T}{2}, \frac{T}{2} + t_r\right) , \qquad x_1 = a \cos \omega t - \frac{f F_N}{k} \qquad t \in \left(\frac{T}{2} + t_r, T\right) . \tag{39}$$

Time histories of $x(t)$ and $x_1(t)$ are shown in Fig. 25, where $T = 2\pi/\omega$.
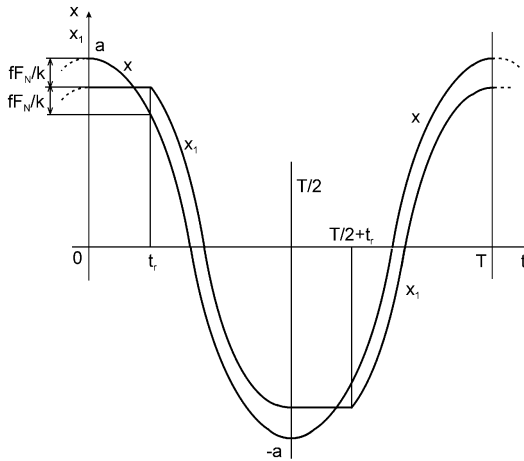

Fig.25

Threshold time τ_r between stick phase and slip phase of motion in the surface is given by

$$x = a \cos \omega t_r = a - 2 \frac{f F_N}{k} = a - 2\Delta , \tag{40}$$

from which

$$\tau_r = \omega t_r = \arccos\left(1 - 2 \frac{f F_N}{k a}\right) . \tag{41}$$

Let us label the non-dimensional expression $f F_N/(k a)$ by ψ:

$$\psi = \frac{f F_N}{k a} . \tag{42}$$

This non-dimensional variable contains all important physical quantities typical for spring-friction connection. Another non-dimensional variable is $\tau = \omega\, t$.

Time history of friction force F_t in contact surfaces is (with an opposite sign) identical with force F_t acting body I and it is ascertained by deformation $f\, F_N / k$ of spring with stiffness k

$$
\begin{aligned}
F_t &= k\, a(\cos\tau - 1 + \psi) & \tau &\in (0, \tau_r)\ , \\
F_t &= -k\, a\, \psi = -f\, F_N & \tau &\in (\tau_r, \pi)\ , \\
F_t &= k\, a(\cos\tau + 1 - \psi) & \tau &\in (\pi, pi + \tau_r)\ , \\
F_t &= k\, a\, \psi = f\, F_N & \tau &\in (\pi + \tau_r, 2\pi)\ ,
\end{aligned}
\tag{43}
$$

where $\tau_r = \arccos(1 - 2\,\psi)$.

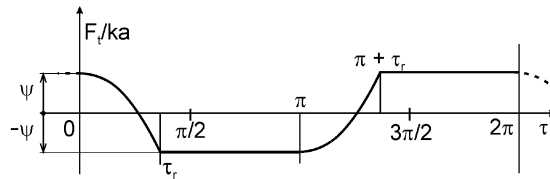The course of friction force is shown in Fig. 26.

Fig.26

Replacing nonlinear function $F(t)$ by an equivalent linear expression is at spring-friction system more complicated than at Coulomb friction. The stiffness and damping components of system in Fig. 24 have to be considered and therefore beside equivalent damping $b_e(a\,\omega)$ also the equivalent linear stiffness $k_e(a)$ [12, 13] must be added to the expression of linearized friction force

$$
F_t = b_e(a\,\omega)\,\dot{x} + k_e(a)\, x\ .
\tag{44}
$$

A parallel model in Fig. 4c replaces a series model in Fig. 4a. Equivalent damping coefficient b_e at assumption

$$
x = a\, \cos\omega t_r\ , \qquad \dot{x} = -a\,\omega\, \sin\omega t\ ,
\tag{45}
$$

is given by [12]:

$$
b_e(a\,\omega) = \frac{-1}{\pi\, a\,\omega} \int_0^{2\pi} F_t(\tau)\, \sin\tau\, \mathrm{d}\tau = \frac{-2}{\pi\, a\,\omega} \int_0^{\pi} F_t(\tau)\, \sin\tau\, \mathrm{d}\tau\ .
\tag{46}
$$

Using (42), (43) gives

$$
\begin{aligned}
b_e(a\,\omega) &= \frac{-2}{\pi\, a\,\omega} \left[\int_0^{\tau_r} k\, a\, (\cos\tau - 1 + \psi)\, \sin\tau\, \mathrm{d}\tau + \int_{\tau_r}^{\pi} -f\, F_N\, \sin\tau\, \mathrm{d}\tau \right] = \\
&= \frac{-2}{\pi\, a\,\omega} \int_0^{\tau_r} k\, a\, \left(\frac{\sin 2\tau}{2} + (-1 + 2\,\psi)\, \sin\tau \right) \mathrm{d}\tau + \frac{2}{\pi\, a\,\omega} \int_0^{\pi} -f\, F_N\, \sin\tau\, \mathrm{d}\tau = \\
&= -\frac{2\, k}{\pi\,\omega} \left[-\frac{\cos 2\tau_r}{4} + (1 - 2\,\psi)\, \cos\tau_r + \frac{1}{4} - 1 + 2\,\psi \right] + \frac{4}{\pi}\, \frac{f\, F_N}{a\,\omega}\ .
\end{aligned}
\tag{47}
$$

Applying $\cos \tau_{\mathrm{r}} = 1 - 2\,\psi$ gives after simple rearrangement

$$b_{\mathrm{e}}(a\,\omega) = \frac{4\,f\,F_{\mathrm{N}}}{\pi\,a\,\omega} \left[1 - \frac{f\,F_{\mathrm{N}}}{k\,a} \right] = b_{\mathrm{e}\infty}\,[1 - \psi] \qquad \text{for} \quad 0 \le \psi \le 1 \ . \tag{48}$$

The limit value $b_{\mathrm{e}\infty} = 4\,f\,F_{\mathrm{N}}/(\pi\,a\,\omega)$ is equivalent linear damping coefficient of a separate dry friction element $(k = \infty)$. The range of dimensionless parameter $\psi \in \langle 0, 1 \rangle$ corresponds to the range of spring stiffness k

$$k \in \left\langle \frac{f\,F_{\mathrm{N}}}{a}, \infty \right\rangle \ . \tag{49}$$

The equivalent linear stiffness $k_{\mathrm{e}}(a)$ of spring-friction system can be ascertained in a similar way:

$$k_{\mathrm{e}}(a) = \frac{1}{\pi\,a} \int\limits_0^{2\pi} F_{\mathrm{t}}(\tau)\,\cos\tau\,\mathrm{d}\tau = \frac{2}{\pi\,a} \int\limits_0^{\pi} F_{\mathrm{t}}(\tau)\,\cos\tau\,\mathrm{d}\tau \ . \tag{50}$$

Introducing $(43), (45)$ gives

$$\begin{aligned}
k_{\mathrm{e}}(a) &= \frac{2}{\pi\,a} \left[\int\limits_0^{\tau_{\mathrm{r}}} k\,a\,(\cos\tau - 1 + \psi)\,\cos\tau\,\mathrm{d}\tau + \int\limits_{\tau_{\mathrm{r}}}^{\pi} -f\,F_{\mathrm{N}}\,\cos\tau\,\mathrm{d}\tau \right] = \\
&= \frac{2\,k}{\pi} \int\limits_0^{\tau_{\mathrm{r}}} \left[\cos^2\tau - (1 - 2\,\psi)\,\cos\tau \right]\,\mathrm{d}\tau = \\
&= \frac{k}{\pi}\,\arccos(1 - 2\,\psi) - \frac{2\,k}{\pi}\,(1 - 2\,\psi)\,\sqrt{\psi\,(1 - \psi)} \ .
\end{aligned} \tag{51}$$

Courses of relative equivalent damping coefficients $b_{\mathrm{e}}(a\,\omega)$ for different stiffness $k = 1 \div 5$ in relation to the equivalent damping $b_{\mathrm{e}\infty}$ of Coulomb friction element (i.e. at infinity stiffness k) are shown in Fig. 27.
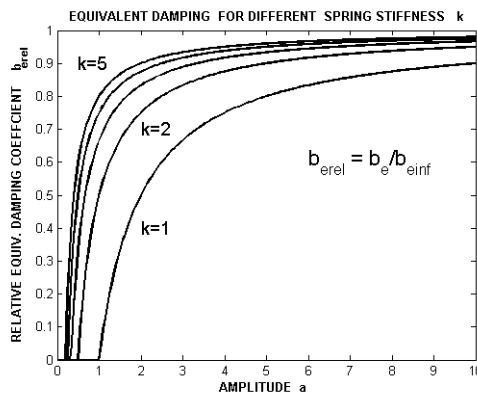

Fig.27

It is evident that with increasing stiffness k the ratio $b_e/b_{e\infty}$ goes to 1 and the properties of spring-friction element approach to the simple dry friction Coulomb element.

The absolute values of equivalent damping b_e in relationship with amplitude a (again for different stiffness $k = 1 \div 5$) are shown in Fig. 28. The equivalent damping for Coulomb friction at $k \to \infty$ is there drawn by a dashed thin hyperbolic curve. Finite values of tangential stiffness k of contact surfaces are depicted by full thick curves. In such a case, zero friction exists at very small amplitudes. This interval of undamped phase $a \in (0, \Delta)$, $\Delta = f\,F_N/k$ decreases with increasing spring stiffness k. After crossing this threshold $a > \Delta$, the equivalent damping b_e suddenly increases, reaches a maximum and then asymptotically decreases again to a zero value. The stronger is the stiffness k, the higher is maximum b_e and the nearer is the property of spring-friction element to the property of Coulomb friction element – dashed curve.
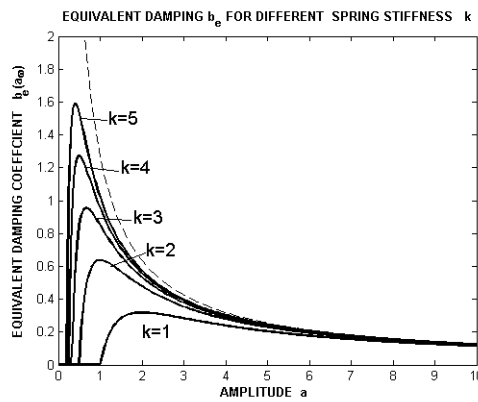

EQUIVALENT DAMPING b_e FOR DIFFERENT SPRING STIFFNESS k

Fig.28

It is evident that the effect of contact tangential stiffness k is worthy of consideration only at very small amplitudes a and/or at very small stiffness k. In other cases, when it approximately holds

$$k\,a > 5\,f\,F_N \ , \tag{52}$$

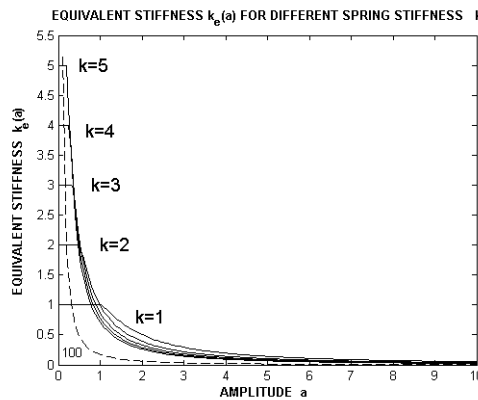it is sufficient and reasonable to use a simple Coulomb model of dry friction.

EQUIVALENT STIFFNESS $k_e(a)$ FOR DIFFERENT SPRING STIFFNESS k

Fig.29

Approximation of spring connection by an equivalent linearized model (44) contains also spring component $k_{\mathrm{e}}(a)\,x$. Let us see how it changes at variable amplitude a. Courses of equivalent stiffness $k_{\mathrm{e}}(a)$ for different stiffness k in the spring-friction element are shown in Fig. 29.

At the undamped vibration $b_{\mathrm{e}}(a\,\omega) = 0$ with small amplitudes

$$a < \frac{f\,F_{\mathrm{N}}}{k} = \Delta \ , \tag{53}$$

the friction force F_{t} contains only elastic component with $k_{\mathrm{e}} = k$. A short horizontal line depicts this phase. For greater amplitudes $a > \Delta$, the equivalent stiffness k_{e} goes quickly to zero, and at $a \cong 5\,\Delta$ it is less than $15\,\%$ of k.

At increasing spring stiffness k the curves $k_{\mathrm{e}}(a)$ move to right, as it is shown by a dashed line for $k = 100$. This curve is for $k \to \infty$ identical with both vertical and horizontal axes and the spring-friction model transfers into simple Coulomb model with no elastic component.

6. Conclusion

The paper presents derivation of analogical relationships of dry friction force versus velocity of relative motion in contact of two bodies. Proceeding from the classical Coulomb law, the varied forms of characteristics are described by analytical or piecewise linear functions. The equivalent linearization method was used to gain simple linear formulae applicable at numerical solution of dynamic properties of machine elements with frictional connections.

Particular attention was paid to the modelling of a stick-slip phenomenon at small amplitudes and velocities of relative motion and both the modified Coulomb law and the spring-friction elements were derived and analysed in detail. The equivalent linearized models are calculated for both types of friction connections. It is shown that the application of the spring-friction models and their linearized approximation is reasonable only for analysing vibrations processes with very small amplitudes and stiffness near the stick phase of motion. For higher amplitudes and stiffness the characteristic of slip phase given by equivalent linear damping is more important and the modified Coulomb friction model and the relevant equivalent linear damping coefficient are sufficient for the solution of most technical systems.

Acknowledgement

References

[1] Sextro W.: Dynamical Contact Problems with Friction, Springer-Verlag 2007, Berlin Heidelberg

[2] Guran A. (ed.): Impact and Friction of Solids, Structures and Intelligent Machines, Series B, Vol. 14, World Scientific 2000, Singapore

[3] Voldřich J.: Modelling of three-dimensional friction contact of vibrating elastic bodies with rough surfaces, Applied and Computational Mechanics 3 (2009) 241–252

[4] Archard J.F.: Contact and Rubbing of Flat Surfaces, Journal of Applied Physics, 24 (1953) 981–988

[5] Pfeifer F., Hajek M.: Stick-slip motion of turbine blade dampers, Phil. Trans. Soc. Lond. A, 338 (1992) 503–517

[6] Koh K.H., et al.: Characterization of Turbine Blade Friction Dampers, Transaction of the ASME, 127 (2005), pp. 856–862

[7] Pŭst L., Pešek L.: Nonlinear Damping in Rotating Disk, In: National Colloquium with International Participation Dynamics of Machines 2010, ed. L. Pešek, IT ASCR, Prague 2010, pp. 63–72

[8] Pŭst L., Pešek L., Veselý J., Radolfová A.: Vliv rozladění nosníků s třecím tlumičem na výšku rezonančních vrcholů, výzkumná zpráva ÚT AV ČR č. Z-1441/09, 2009, Praha

[9] Deoras S.K., Talke F.E.: Effect of Intermolecular Forces on the Dynamic Response of a Slider, Journal of Tribology, 129 (2007) 177–180

[10] Gallego L., Nelias D.: Modeling of Fretting Wear Under Gross Slip and Partial Slip Conditions, Journal of Tribology, 129 (2007) 528–536

[11] Pŭst L.: Tangentialkräfte und transvelsale Microdeformation in den Berührungsflächen von Wälzlagern, Acta Technica ČSAV, 2 (1962) 141–173

[12] Brepta R., Pŭst L., Turek F.: Mechanické kmitání, Sobotáles 1994, Praha

[13] Pŭst L., Tondl A.: Úvod do theorie nelineárních a quasiharmonických kmitů mechanických soustav, ČSAV 1956, Praha

[14] Pŭst L., Pešek L.: Různé typy charakteristik suchého tření, In: National Colloquium with International Participation Dynamics of Machines 2011, ed. L. Pešek, IT ASCR, Prague 2011, pp. 77–78

[15] Gradshtejn I.S., Ryzhik I.M.: Tablicy integralov, summ, rjadov i proizvedenij, Izd. Nauka 1971, Moskva

Note: This paper is an extended version of the contribution presented at the national colloquium with international participation *Dynamics of Machines 2011* in Prague.